

TIME-FREQUENCY ANALYSIS AND MODAL BEHAVIOR FROM AIRGUN SIGNALS IN SHALLOW WATER

H. Dong, Norwegian University of Science and Technology, Trondheim, Norway
M. Badiey, University of Delaware, Newark, Delaware, US
N. R. Chapman, University of Victoria, Victoria, B.C. Canada
email: hefeng@iet.ntnu.no

1 INTRODUCTION

Internal waves have pronounced impacts on sound propagation and sound intensity in shallow water that have been studied theoretically and experimentally.¹⁻⁶ Sound intensity experiences focusing and defocusing fluctuation when the leading front of an internal wave is nearly parallel to and passes through the source-receiver track. The phenomenon is due to horizontal refraction causing the sound energy to go out of the source-receiver plane and leads to 3D effects. Furthermore, sound speed fluctuations in the water column due to internal waves cause coupling between propagating acoustic modes.

In this paper, broadband acoustic signals recorded in experiments at a shallow water region of the New Jersey Shelf are analyzed to study the influence of internal waves on sound propagation, sound intensity and modal structure. Modal behavior and fluctuations due to sound intensity focusing and defocusing are presented. A mode filtering technique, the time warping transform, is applied to resolve modes for the frequency band of 20-180 Hz. The remainder of this paper is organized as follows. Section 2 describes data collection including oceanographic information. Section 3 presents the time-frequency analysis and warping transform to resolve the propagating modes. Section 4 gives a discussion and summary.

2 EXPERIMENTAL OBSERVATIONS

The SWARM experiment was conducted in the Mid-Atlantic Bight on the continental shelf region off the coast of New Jersey in the summer of 1995.¹ The data used in this paper were recorded in a subexperiment between 19:00 and 20:00 GMT on August 4. The data were collected by a WHOI Vertical Line Array (VLA) with 16 hydrophones evenly spaced at 3.5 m from 14.9 to 67.4 m below the sea surface. The data were generated by an airgun source at 12 m below the sea surface and 15 km from the receiving array. The airgun source was fired at a rate of 1 minute. The water depth along the source-receiver track is almost constant at around 72 m. A thermistor chain spanned the water column at the WHOI VLA location was deployed to measure temperature variation during the experiment. The temperature was recorded every 30 seconds. The top panel in Figure 1 shows the thermistor data during a one-hour period from 19:00 to 20:00 GMT on August 4. Badiey et. al.¹ showed that during this period an internal wave packet was passing through the WHOI VLA. Due to internal wave passage, the thermistor data fluctuate near the water surface layer of 20-25 m, and as the depth increases the temperature data approach a constant value. Moreover, it is seen that the temperature fluctuations have a period of approximate 12-15 minutes. The bottom panel in Figure 1 plots the sound speed profile generated from the thermistor data. It is clear that the sound speed in the upper part of the water column fluctuates which influences sound propagation and mode structure. Sound intensity influenced by internal waves experiences focusing and defocusing. Two events marked by red and black lines in Figure 1 corresponding to the sound intensity focusing and defocusing are selected for study of modal behavior and mode structure.

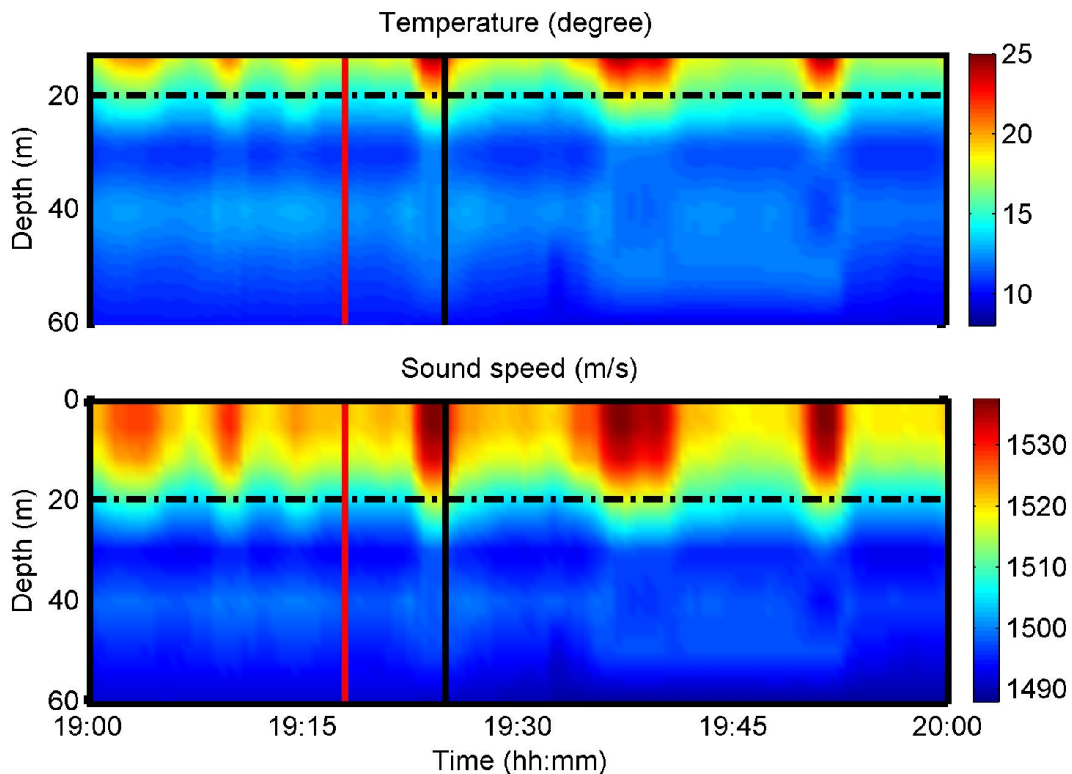


Figure 1. Top: Temperature profile measured at the WHOI array location between 19:00-20:00 GMT on August 4, 1995; Bottom: Sound speed profile generated by the temperature profile on top panel. The red and black lines correspond to the events when sound intensity experiences focusing and defocusing.

3 TIME-FREQUENCY ANALYSIS

The data from 16 hydrophones for intensity focusing and defocusing events are analyzed. Sound intensity fluctuation during the same period of one hour is presented on the top panel of Figure 2, illustrating the focusing and defocusing phenomenon. The selected two events are denoted by the red and black lines. The spectrograms of the two events for a selected hydrophone are presented on the bottom panels in Figure 2: focusing event on the left and defocusing event on the right. It is evident that the modal structures of the two cases are more or less the same. However, the energy levels of the modes are very different. In the defocusing event the acoustic energy is pulled out of the source-receiver plane by horizontal refractions.⁴⁻⁶

The envelope of the signals for different depths is presented in Figure 3 for the focusing (left) and defocusing (right) events. The signals are obtained by using 10-Hz narrow band filters on the broad band signals with a carrier frequency of 60 Hz. Three modes are shown in both cases. However, mode 2 in the defocusing event is distorted and very weak compared with that in the focusing event.

In order to separate the modes and extract the mode spectrum and dispersion curves, a mode filtering technique, time warping⁷, is applied to single hydrophone data. The warped signal $y_w(t)$ is obtained by warping transform on a given signal $y(t)$:

$$y_w(t) = \sqrt{|w'(t)|} y[w(t)], \quad (1)$$

where $w(t)$ is warping function and $w'(t)$ is the derivative of $w(t)$. The warping function is defined as

$$w(t) = \sqrt{t^2 + t_r^2}, \quad t_r = r / c_w \quad (2)$$

where r is the source-receiver distance and c_w is the water sound speed. The warping transform is invertible. The transformation is adapted to an ideal iso-speed waveguide with a rigid bottom and it is robust and can be applied to most low-frequency shallow water scenarios.^{8,9} By applying this transform to single hydrophone data dispersed modes can be extracted.

Figure 4 illustrates an example of the warping transform. Single hydrophone data from the focusing event (top left) are transformed to a warped signal (top right). Its representation in the warped time-frequency domain is shown in the bottom right where the warped modes are separated. The resolved modes are then filtered and unwarped to the original time domain using the inverse function $w^{-1}(t)$ to obtain the mode spectrum and dispersion curves.⁷ This procedure is applied to 16-hydrophone data for the two events. Figure 5 shows the estimated dispersion curves based on the results from the 16 hydrophones by the warping procedure for the focusing (left) and defocusing (right) events. Four modes in the frequency band 20–180 Hz are extracted for the focusing event, while only three modes in the frequency band 20–100 Hz are extracted in the defocusing event.

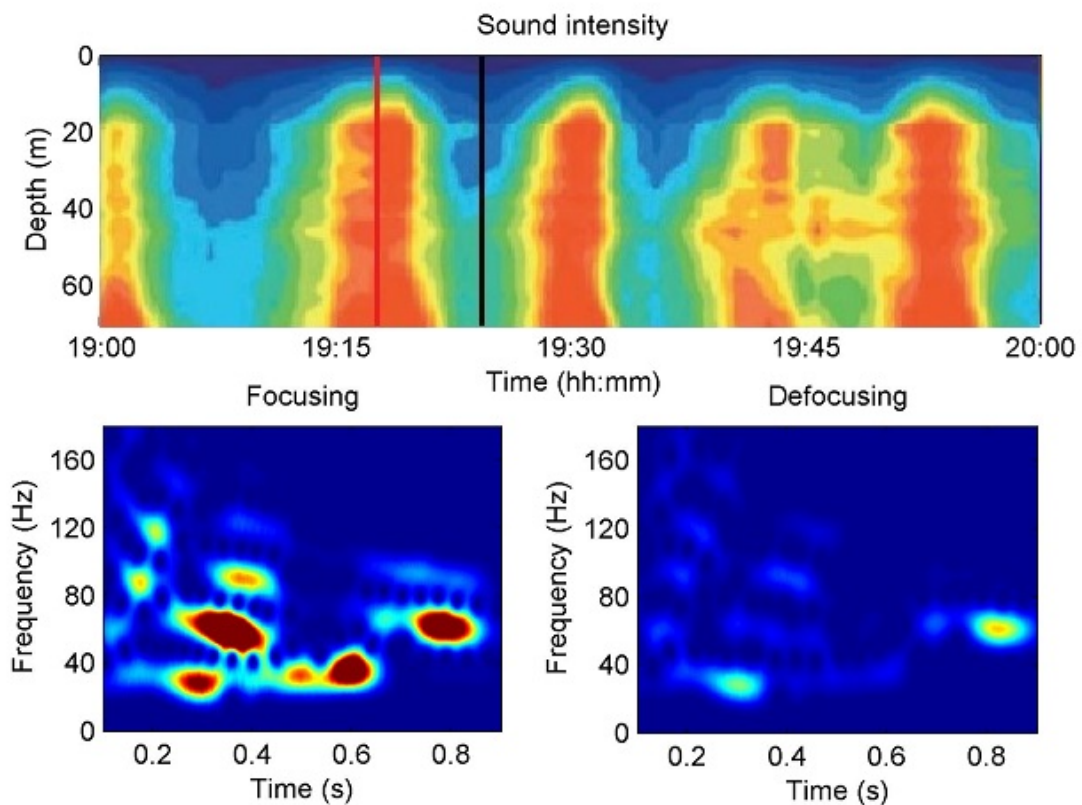


Figure 2. Top: Fluctuation of sound intensity measured at the WHOI array in the period of 19:00–20:00 and two selected events of focusing (red) and defocusing (black). Bottom: Spectrogram for the events of focusing (left) and defocusing (right) defined in the top panel.

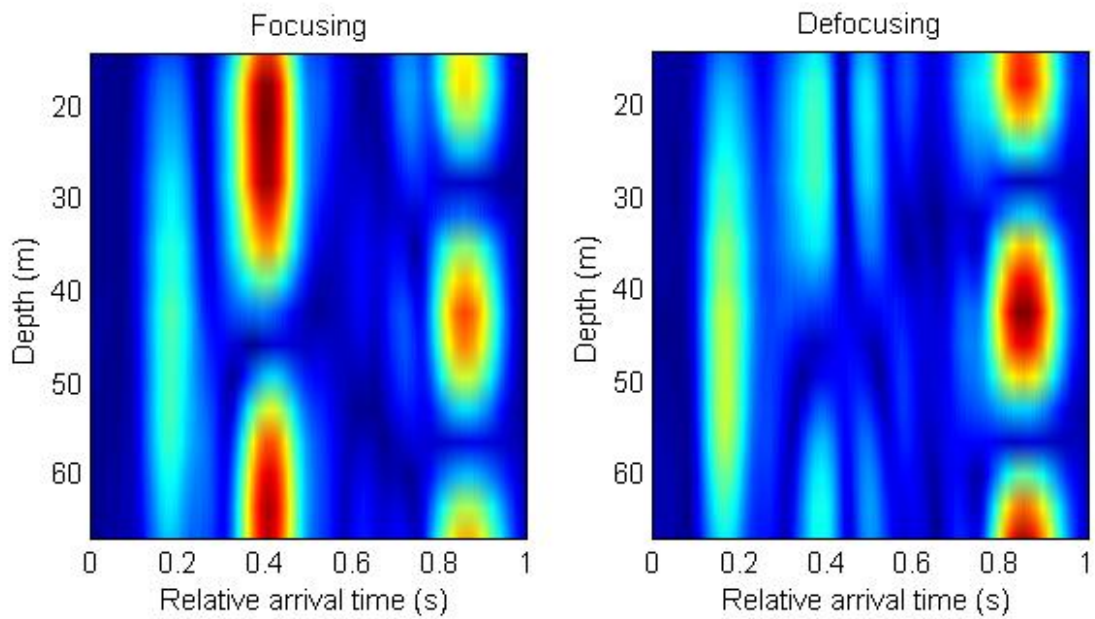


Figure 3. Envelope of the signals at different depths for the focusing (left) and defocusing (right) events.

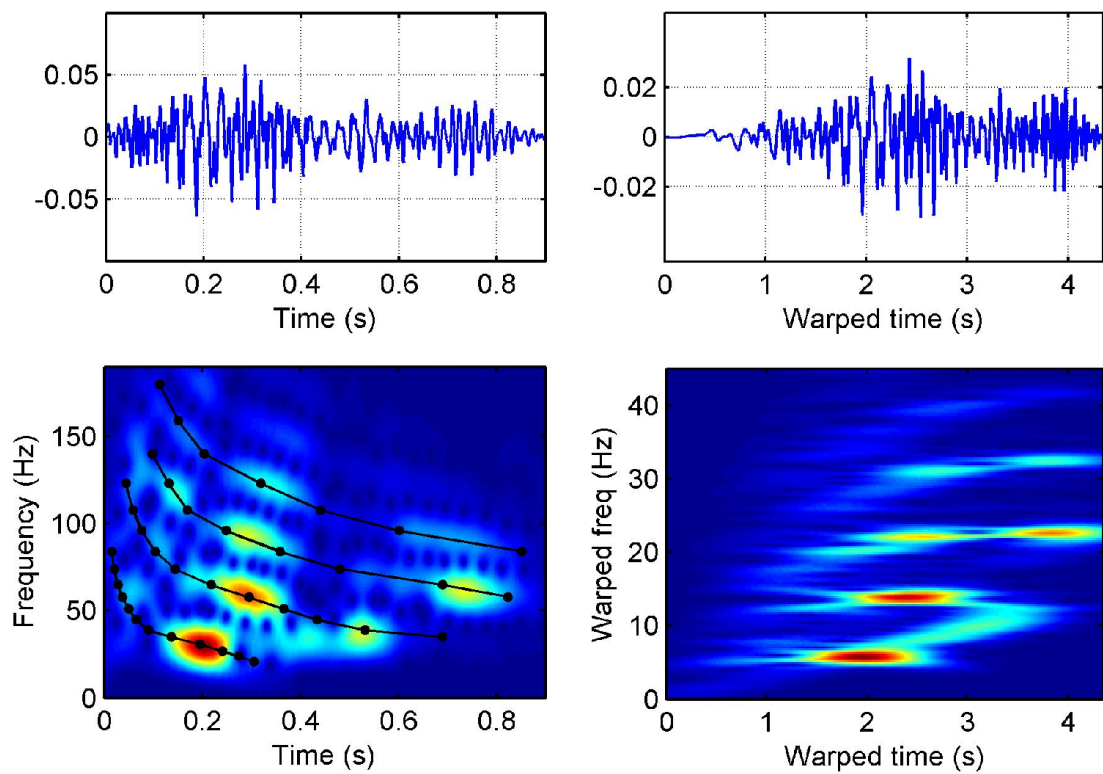


Figure 4. Example of the warping transform. Upper left: received signal; Upper right: warped signal; Bottom right: spectrogram in warping domain; Bottom left: spectrogram of the original signal and extracted dispersion modes (black curves with dots).

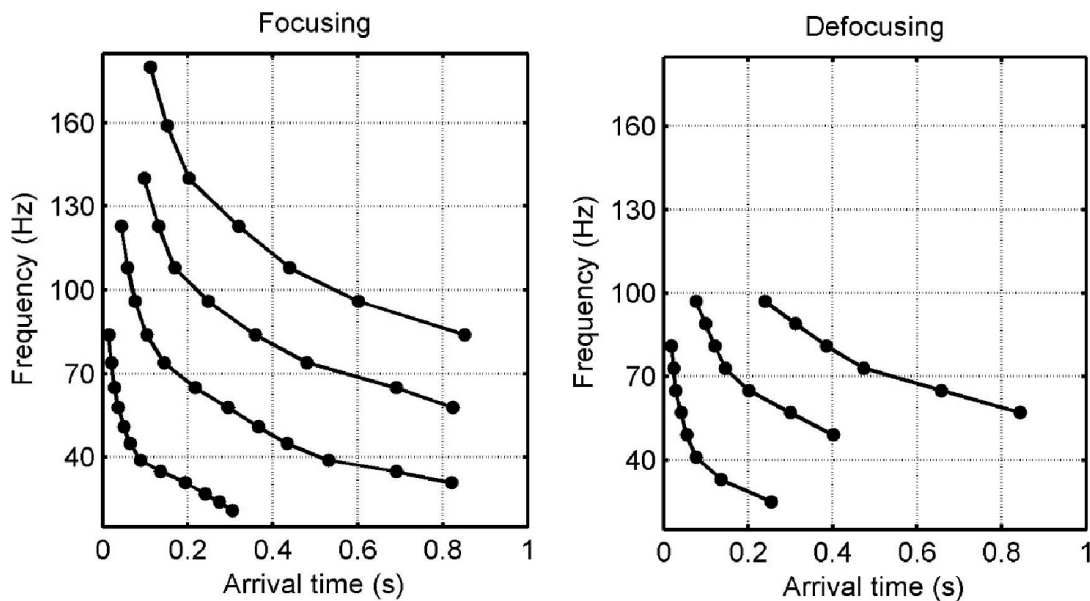


Figure 5. Extracted dispersion curves based on the results from the 16 hydrophones and sampled points (dots). Left: focusing event; Right: defocusing event.

4 DISCUSSION AND SUMMARY

Spatial and temporal variation of water column properties due to internal waves in shallow water can have significant impact on sound propagation, sound intensity and modal behavior. The sound intensity fluctuation due to the internal waves is intuitive as shown on the top panel of Figure 2. However, the impact on modal behavior and dispersion characteristics needs to be analyzed using an advanced time-frequency technique. The results of the analysis demonstrate that the variation in the sound propagation environment has a strong impact on the modal behavior and dispersion structure. The dispersion curves extracted using the warping procedure for focusing and defocusing events are different both in the number of modes and the frequency band. If these results were used in geoacoustic inversion to estimate seabed acoustic properties, different estimates would be obtained for the same sea bottom environment. Since internal waves are present in many coastal shelf environments, the analysis presented here brings into question on the validity of geoacoustic inversion results that are obtained without detailed analysis of the conditions in the water column. The influence on geoacoustic inversion will be investigated in future work.

5 REFERENCES

1. M. Badiey, Y. Mu, J. F. Lynch, J. Apel, and S. Wolf, Temporal and Azimuthal Dependence of Sound Propagation in Shallow Water With Internal Waves, *IEEE J. Ocean Eng.* **27**(1), 117-129, (2002).
2. M. Badiey, B. Katsnelson, J. F. Lynch, S. Pereselkov, and W. Siegmann, Measurement and modeling of 3-D sound intensity variations due to shallow water internal waves, *J. Acoust. Soc. Am.* **117**, 613-625 (2005).
3. S. H. Weinberg and R. Burridge, Horizontal ray theory for ocean acoustics, *J. Acoust. Soc. Am.* **55**, 63-79 (1974).

4. S. D. Frank, M. Badiey, and W. Siegmann, Experimental evidence of three-dimensional acoustic propagation caused by nonlinear internal waves, *J. Acoust. Soc. Am.* **118**(2), 723-734 (2005).
5. B. G. Katsnelson and S. Pereselkov, Low-frequency horizontal acoustic refraction caused by internal wave solitons in a shallow sea, *Acoust. Phys.* **46**, 684-691 (2000).
6. M. Badiey, B. G. Katsnelson, J. F. Lynch and S. Pereselkov, Frequency dependency and intensity fluctuations due to shallow water internal waves, *J. Acoust. Soc. Am.* **122**(2), 747-760 (2007).
7. J. Bonnel and N. R. Chapman, Geoacoustic inversion in a dispersive waveguide using warping operators, *J. Acoust. Soc. Am.* **130**, EL101-EL107 (2011).
8. J. Bonnel, B. Nicolas, J. Mars, and S. Walker, Estimation of modal group velocities with a single receiver for Geoacoustic inversion in shallow water, *J. Acoust. Soc. Am.* **128**, 719-727 (2010).
9. J. Bonnel, C. Gervaise, P. Roux, B. Nicolas, and J. Mars, Modal depth function estimation using time-frequency analysis, *J. Acoust. Soc. Am.* **130**, 61-71 (2011).